Geosciences Journal
Vol. 10, No. 4, p. 465 − 477, December 2006

Q-values for P and S waves in the southern Korean Peninsula based on the coda-normalization method

Sung Kyun Kim, Jae Yol Yang — *School of Earth Systems and Environmental Sciences, College of Natural Sciences, Chonnam National University, Kwangju 500-757, Korea*
Jinyong Oh* — *Nondestructive Research Laboratory of Cultural Properties, Kongju National University, Kongju 314-710, Korea*

ABSTRACT: The attenuation of seismic waves can be measured by the quality factor Q, which is an important parameter of the physical properties of the Earth's interior. Using the extended coda-normalization method, we estimated Q-values for P waves (Q_P) and S waves (Q_S) in the southern Korean Peninsula as well as for the three sub-tectonic provinces (the Gyeonggi Massif, the Ogcheon Belt and the Yeongnam Massif, and the Gyeongsang Basin) in it. We chose 675 seismograms from 189 earthquakes that occurred in Korea from January 2001 to October 2003. Most earthquakes had small magnitudes ($M_L \leq 3.0$) and shallow focal depths (≤15 km). Assuming that Q is independent of frequency, the Q-value and geometric spreading factor (γ) were calculated simultaneously using least squares inversion. The resulting values for the southern Korean Peninsula were Q_P=1384 and Q_S=2036. The Gyeongsang Basin had the lowest value, indicating that its crustal structure is relatively heterogeneous and might be highly fractured. The γ values varied from 0.73 to 0.87. Assuming that Q is dependent on frequency and γ has a constant value of 1.0, the values of Q at the central frequencies of 1, 2, 3, 5, 10, 20, and 30 Hz yielded Q_P=188.6 $f^{0.8110}$ and Q_S=201.4 $f^{0.7509}$ for the southern Korean Peninsula. We analyzed the variation of Q_S for two hypocentral distance ranges: 0–90 km and 90–180 km, respectively. The estimated Q-values for both P and S waves in the Gyeongsang Basin are the lowest, except for the case of $Q_S(f)$, in the low frequency range. The frequency-dependent Q_S for the hypocentral distance range of 90 to 180 km appeared to be the larger than that for the shorter distance range. The values of $Q_S(f)$ estimated in this study were comparatively higher than for a seismically active area.

Key words: coda normalization, geometric spreading factor, P wave, Q-value, S wave, sub-tectonic provinces

1. INTRODUCTION

In general, earthquake ground motion results from the combined effects of the seismic source, the physical properties of the medium, and the site characteristics beneath the recording station. Seismic waves decrease in amplitude as they propagate. This phenomenon is caused by the geometric spreading of the wave front and the absorption of seismic energy due to internal friction or anelasticity. The dependence of amplitude decay on internal friction is referred to as attenuation and is an important property for defining the characteristics of the medium. Attenuation of a seismic wave is measured by a dimensionless parameter known as the quality factor Q. Generally, attenuation depends on the frequency of the seismic waves, and thus Q is expressed as a function of the frequency f as follows: $Q = Q_0 f^n$, where Q_0 and n are constants varying from region to region depending on the attenuation characteristics of the seismic waves (Aki and Chouet, 1975). The study of Q provides valuable information about the Earth's interior and is essential in engineering seismology and in predicting the effects of strong ground motion.

Several researchers have reported the Q-values for P wave (Q_P) and S wave (Q_S) in the southern Korean Peninsula (Chung and Sato, 2000, 2001a, 2001b; Chung et al., 2001; Kim et al., 1999; Kim et al., 2000; Kim et al. 2004). However, most of these studies have been performed in the Gyeongsang Basin, the location of numerous industrial facilities, including nuclear power plants. Because safety and earthquake hazard evaluations are critical in this region, the Korea Institute of Geoscience & Mineral Resources (KIGAM) has operated a digital seismic network in the Gyeongsang Basin since 1995.

Kim et al. (1999) first analyzed the Q-value for P waves in the southern Korean Peninsula using the spectral ratio of P and S waves. In addition, Kim et al. (2000) calculated Q_P from the initial pulse width of the first P motion (Stacey et al., 1975). For ray paths across the major fault line, Q_P-values appeared to be significantly lower than those along the major fault line. A one-dimensional Q_S structure with the depth in the Gyeongsang Basin corresponding to its seismic velocity model was proposed by Kim et al. (2000). Chung and Sato (2000; 2001a) estimated Q_P and Q_S in the Gyeongsang Basin by using the extended coda-normalization method (Yoshimoto et al, 1993) which was originally proposed by Aki (1980). By comparing the results obtained for the Gyeongsang Basin with those obtained in the other regions with variable seismicities in other country, Chung and Sato (2000; 2001a) concluded that the values of Q_P and Q_S in the Gyeongsang Basin are coincident with those of a seismically stable area.

Since 1999, KIGAM and the Korea Meteorological

*Corresponding author: class@kongju.ac.kr

Administration (KMA) have deployed digital seismic networks nationwide. The accumulated data allow us to study Q-values for the various tectonic provinces of the Korean Peninsula. In addition, the large volume of records can be used to re-examine Q-values found by previous studies. The purpose of the present study is to estimate the values of Q_P and Q_S for the three sub-tectonic provinces, the Gyeonggi Massif, the Ogcheon Belt and the Yeongnam Massif, and the Gyeongsang Basin, in the southern Korean Peninsula using the extended coda-normalization method.

2. EARTHQUAKE DATA

The major organizations involved in earthquake observations in Korea are the KMA and KIGAM. For this study, we selected short-period and broadband velocity seismograms recorded by the KMA and KIGAM networks from January 2001 to October 2003. The 675 seismograms from 189 local earthquakes of which origin time and location are shown in Appendix 1 were selected. The selected seismograms had high signal-to-noise (S/N) ratios. Figure 1 shows the distribution of the ray paths between the epicenters and stations. The hypocentral distances for the selected earthquakes ranged from 0 to 180 km (Fig. 2a). Beyond this distance, it is difficult to identify phases such as Sg, SmS, and Lg. Also, in the vicinity of the 60-sec lapse time, Lg and surface waves overlapped with coda waves. Most of the earthquakes had focal depths less than 15 km (Fig. 2b). Magnitudes ranged between 1.5 and 4.5, with more than 60% of the magnitudes centered from 2.0 to 3.0 (Fig. 2c).

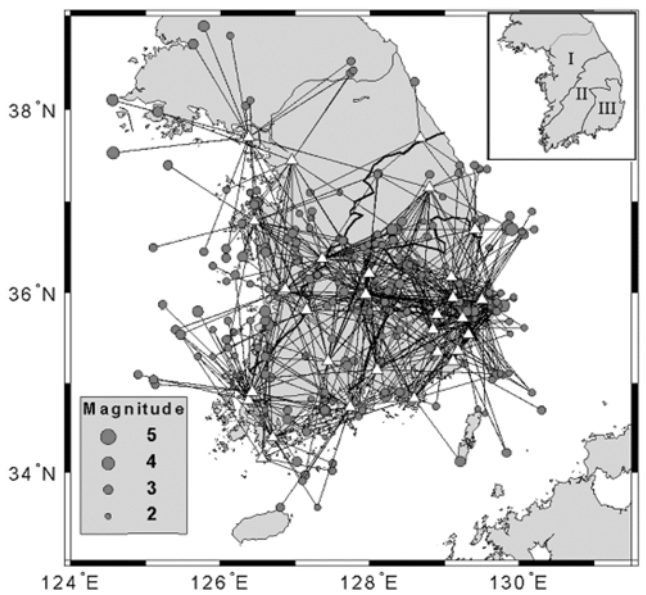

Fig. 1. Distribution of ray paths (lines) between earthquakes (circles) and stations (white triangles). The inset map denotes the tectonic divisions of the southern Korean Peninsula. I: Gyeonggi Massif; II: Ogcheon Belt and the Yeongnam Massif; III: Gyeongsang Basin.

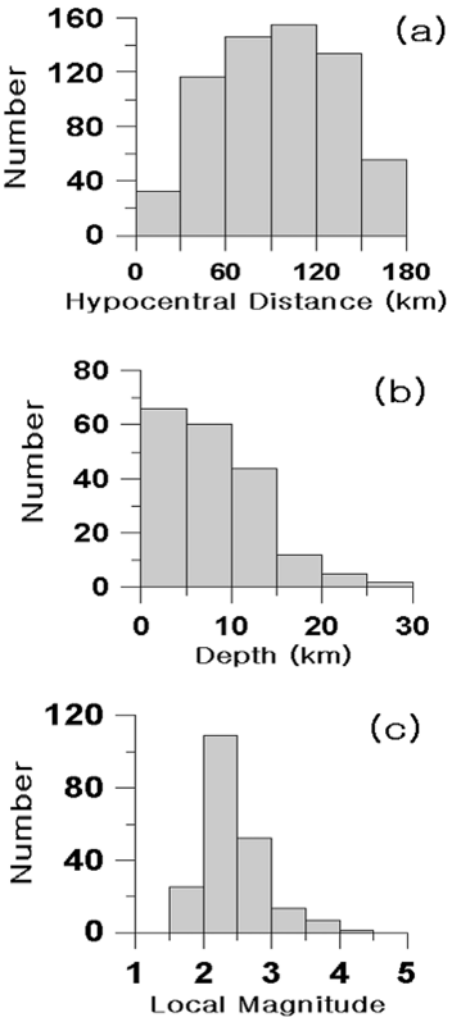

Fig. 2. Distributions of the (a) hypocentral distance, (b) depth, and (c) local magnitude of the earthquakes used in this study.

To compare the attenuation characteristics of P and S waves among the sub-tectonic provinces in the southern Korean Peninsula, we divided the Peninsula into three distinct blocks, with reference to the method of Reedman and Um (1975). As shown in the inset map in Figure 1, these blocks are the Gyeonggi Massif, the Ogcheon Belt and the Yeongnam Massif, and the Gyeongsang Basin. We classified the ray paths by the epicenter located within a block and by the traversing distance at least two-thirds of the block. We selected 54 earthquakes and 95 ray paths for the Gyeonggi Massif, 72 earthquakes and 175 ray paths for the Ogcheon Belt and the Yeongnam Massif, and 74 earthquakes and 243 ray paths for the Gyeongsang Basin. For the entire southern Korean Peninsula, we examined 189 earthquakes with 675 ray paths, regardless of the location of the epicenter and its ray path.

3. METHODS

To analyze the regional characteristics of seismic attenuation in the southern Korean Peninsula, we used the coda-normalization method by which the Q-values for both P and S waves can be estimated. Coda waves consist of the waves scattered by the heterogeneous part within the Earth's interior (Aki and Chouet, 1975). Because the spectral amplitudes of P and S waves are normalized by the amplitude of the coda wave within a fixed lapse time, the Q-value for P and S waves can be obtained even from a seismogram made by a single station.

The coda-normalization method used in this study is perfectly the same as that of Yoshimoto et al. (1993). According to the theory in the paper, the spectral amplitude ratio of the body wave (P or S) and the coda wave can be represented by

$$A_i(f_j, R_i) = -\frac{\pi f_j R_i}{QV} - \gamma \ln R_i + const(f_j) \quad (1)$$

where $A_i(f_j, R_i) = \langle \ln[\frac{A_P(f,R)}{A_C(f,t_C)}] \rangle_{R\pm\Delta R}$ or $\langle \ln[\frac{A_s(f,R)}{A_C(f,t_C)}] \rangle_{R\pm\Delta R}$. $A_P(f, R)$ and $A_s(f, R)$ indicate spectral amplitudes of the P and S waves, respectively, at the frequency f and at the hypocentral distance R. $A_c(f, t_c)$ indicates the coda spectral amplitude at the lapse time t_c. Also, $A_i(f_j, R_i)$ represents the average value of the logarithmic spectral ratio for the j-th frequency and i-th earthquake at hypocentral distance between R and $R\pm\Delta R$. Q, and V are the Q-values and the velocities of the P and S waves, respectively. γ is the geometrical spreading factor of body waves and $const(f_j)$ represents a term related with the coda wave excitation for the j-th frequency but is independent of the hypocentral distance. The solution for Equation (1) can be obtained from the system of linear equations in the following matrix expression:

$$\begin{vmatrix} -\pi f_1 R_1 & -\ln R_1 & 1 & 0 & 0 & \cdots & 0 \\ -\pi f_1 R_2 & -\ln R_2 & 1 & 0 & 0 & \cdots & 0 \\ -\pi f_1 R_3 & -\ln R_3 & 1 & 0 & 0 & \cdots & 0 \\ \vdots & \vdots & \vdots & \vdots & \vdots & \cdots & \vdots \\ -\pi f_1 R_M & -\ln R_M & 1 & 0 & 0 & \cdots & 0 \\ -\pi f_2 R_1 & -\ln R_1 & 0 & 1 & 0 & 0 & 0 \\ -\pi f_2 R_2 & -\ln R_2 & 0 & 1 & 0 & 0 & 0 \\ \vdots & \vdots & \vdots & \vdots & \vdots & \cdots & \vdots \\ -\pi f_2 R_M & -\ln R_M & 0 & 1 & 0 & 0 & 0 \\ \vdots & \vdots & \vdots & \vdots & \vdots & \cdots & \vdots \\ -\pi f_j R_i & -\ln R_i & 0 & 0 & 0 & 1 & 0 \\ \vdots & \vdots & \vdots & \vdots & \vdots & \cdots & \vdots \\ -\pi f_j R_M & -\ln R_M & 0 & 0 & 0 & 0 & 1 \end{vmatrix} \begin{vmatrix} 1/QV \\ \gamma \\ b_1 \\ b_2 \\ b_3 \\ \vdots \\ b_j \\ \vdots \\ b_N \end{vmatrix} = \begin{vmatrix} A_1(f_1, R_1) \\ A_2(f_1, R_2) \\ A_3(f_1, R_3) \\ \vdots \\ A_M(f_1, R_M) \\ A_1(f_2, R_1) \\ A_2(f_2, R_2) \\ \vdots \\ A_M(f_2, R_M) \\ \vdots \\ A_i(f_j, R_i) \\ \vdots \\ A_M(f_N, R_M) \end{vmatrix} \quad (2)$$

where $b_j = const(f_j)$, M is the number of earthquakes, and N is the number of frequency bands. By the least squares inversion method, we can obtain γ and Q-values for P or S waves, simultaneously.

In this study, we calculated the Q-values for P and S waves using two different ways described below. In the first method, the values of γ, Q_P, and Q_S were simultaneously estimated by assuming that Q is independent of the frequency. In the second method, Q_P and Q_S were estimated by assuming that γ has a constant value of 1. Consequently, the second term of the right-hand side of Equation (1) also becomes a constant. Then, when the left-hand side of Equation (1) is plotted with respect to the hypocentral distance, the Q-value for P and S waves at frequency f are obtained from the slope of the regression line. In estimating Q_P and Q_S from Equations (1) and (2), V_p and V_s are assumed to be 6.0 and 3.4 km/sec, respectively, referring to Kim (1995).

4. DATA PROCESSING

The seismograms consist of three-component data recorded at a rate of 100 samples per second. Both the up–down (U–D) component for P waves and the north–south (N–S) component for S waves were chosen. If the N–S component was disqualified, it was replaced by its corresponding east–west (E–W) component. However, in most cases we used the N–S component seismogram. As the first step in preprocessing the raw data, the DC offset from the zero level and linear trend of the original seismogram were removed. Then a 10% cosine tapering function was applied to the beginning and end of the data using the method of Hino (1986). To estimate the frequency-dependent Q-value, the seismograms were band-pass filtered at the central frequencies (f_0) of 1, 2, 3, 5, 10, 20, and 30 Hz using a six-pole Butterworth band-pass filter with a bandwidth of $1/\sqrt{2}\ f_0 \sim \sqrt{2}\ f_0$.

The 5-sec time window for P and S waves in the filtered seismograms was designed from the beginning of the waves (P or S). Their spectral amplitudes in each filtered seismogram were determined using one-half of the maximum peak-to-peak amplitude within the time window. The spectral amplitude of the coda wave was assumed to be the root mean square (RMS) of the amplitude of the seismic wave within the 5-sec time window after the 60-sec lapse time.

Figure 3 shows an example of the N-S component raw and filtered seismograms with time windows for P, S, and coda waves. For data with short hypocentral distances, the P-wave time window was reduced when the time difference between P and S wave arrival times was less than 5 sec. The S-wave time window was also reduced in cases where the hypocentral distance was long and the SmS phase was included in the window. Then, data having S/N ratios greater than 2 were selected in each frequency. The hypocentral distance R was calculated from the epicentral distance (R_0) and the focal depth (h) using the relationship $R = \sqrt{R_0^2 + h^2}$.

5. RESULTS

We determined unknown values of Q and γ in Equation

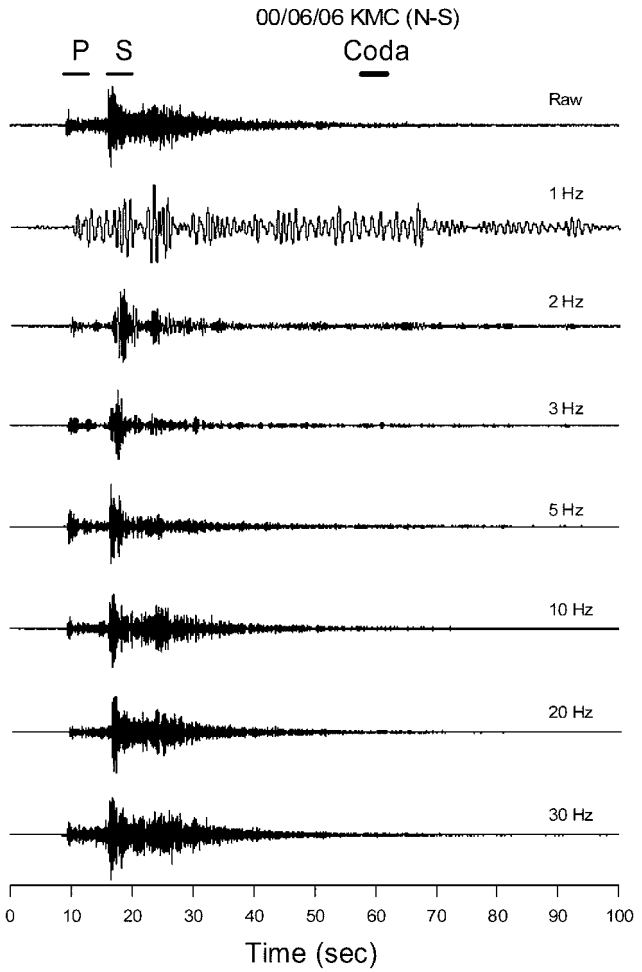

Fig. 3. An example of recorded and its band-pass filtered seismograms. A N–S component short period seismogram recorded at the KMC station is shown at the top. The horizontal bars represent the time windows for the P, S, and coda waves. Seven band-pass-filtered seismograms for central frequencies at 1, 2, 3, 5, 10, 20, and 30 Hz are displayed below.

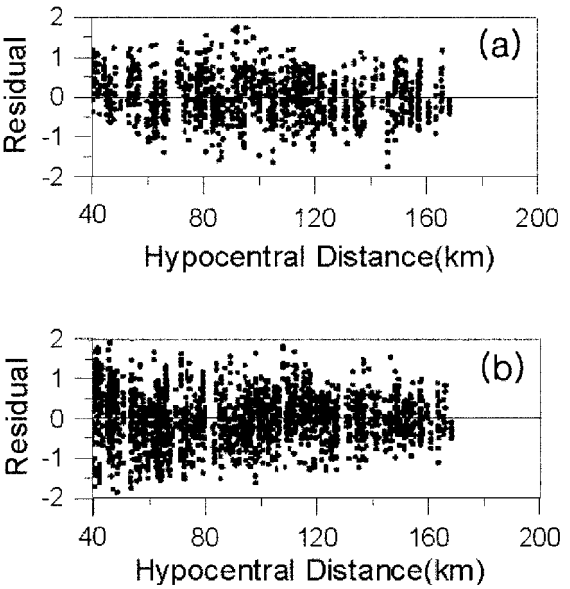

Fig. 4. Residuals in log units of the regression after inversion for Q_P (a) and Q_S (b).

(2) by assuming that γ is a constant for all distances. In Figure 4, the residuals between the normalized values for the observed P and S wave data and the theoretical values calculated from the inversion confirm the reliability of the inversion results. The lack of correlation between the residuals ranging from -2.0 to 2.0 and the hypocentral distances indicate that the inversion result is reasonable.

Table 1 summarizes the estimated frequency-independent values of Q_P, Q_S, and γ. For the whole southern Korean Peninsula, Q_P and Q_S are 1384 and 2036, respectively, and the value of Q_S/Q_P is approximately 1.47. Table 1 also shows the values of Q_P and Q_S for the sub-tectonic provinces. The Q_S value for the whole southern Korean Peninsula exceeds any of sub-tectonic province Q value. This fact implies that rays across the whole southern Korean Peninsula have more possibilities to penetrate the deeper part of the earth. The γ values obtained for the sub-tectonic provinces range from 0.73 to 0.86. It must be noted that the γ values obtained here range between 1.0 and 0.5, as expected for body waves and for surface waves, respectively.

The frequency-dependent values of Q_P and Q_S were calculated at seven pass bands (1, 2, 3, 5, 10, 20, and 30 Hz) with a fixed value of $\gamma=1$ by the second method described in the previous section. Then, Q_P and Q_S were assumed to be a function of the form of the power law for the frequency (f). The best fit functions $Q_P(f)$ and $Q_S(f)$ for the sub-tectonic provinces and for the whole southern Korean Penin-

Table 1. Summary of the estimated frequency-independent Q-value and geometrical spreading factor (γ) for the southern Korean Peninsula and its three sub-tectonic provinces.

Parameters		Tectonic Province			
		Gyeonggi Massif	Ogcheon Belt & Yeongnam Massif	Gyeongsang Basin	Southern Korean Peninsula
P wave	Q	1455	1307	1112	1384
	γ	0.83	0.87	0.84	0.83
S wave	Q	1868	1899	1828	2036
	γ	0.74	0.73	0.76	0.71

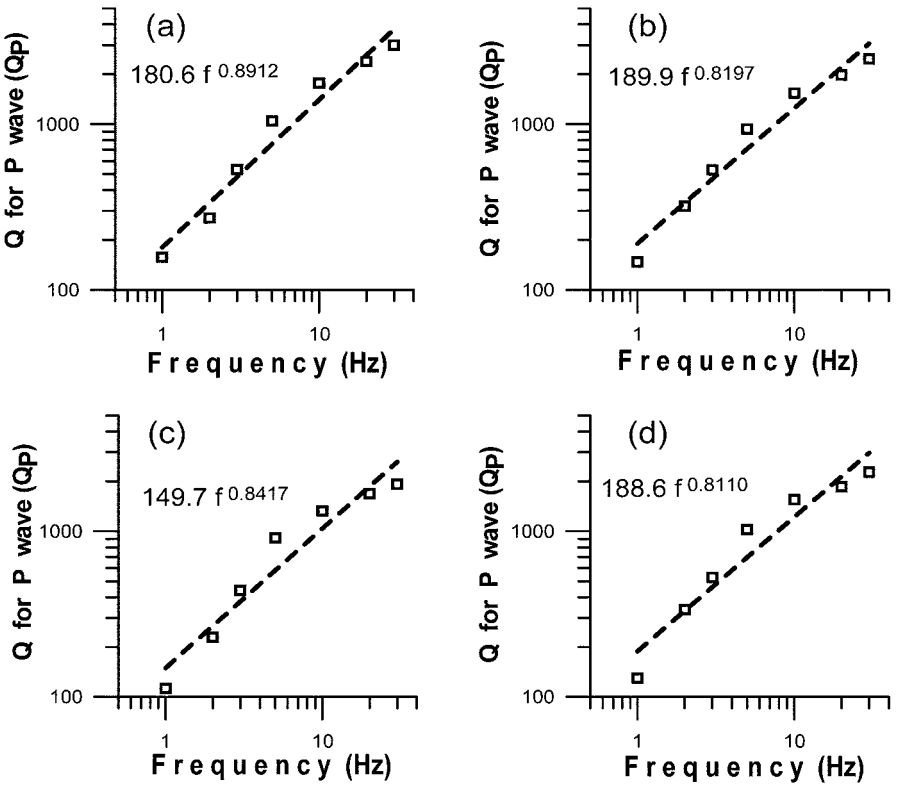

Fig. 5. Frequency-dependent Q_P for (a) the Gyeonggi Massif, (b) the Ogcheon Belt and the Yeongnam Massif, (c) the Gyeongsang Basin, and (d) the entire southern Korean Peninsula.

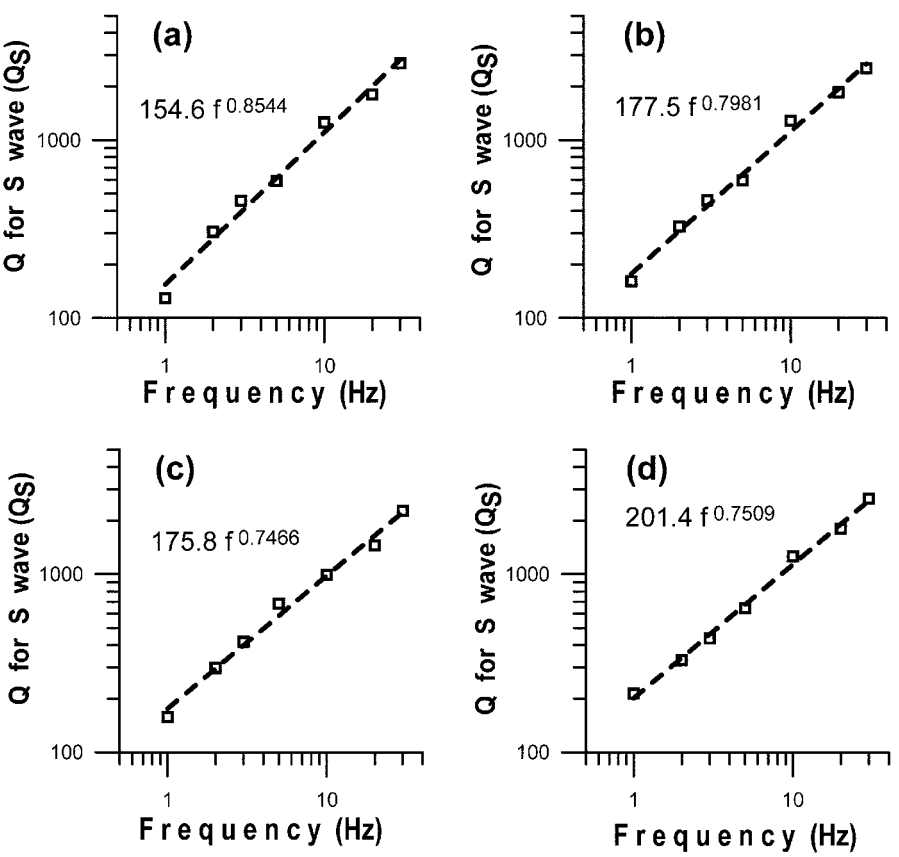

Fig. 6. Frequency-dependent Q_S for (a) the Gyeonggi Massif, (b) the Ogcheon Belt and the Yeongnam Massif, (c) the Gyeongsang Basin, and (d) the entire southern Korean Peninsula.

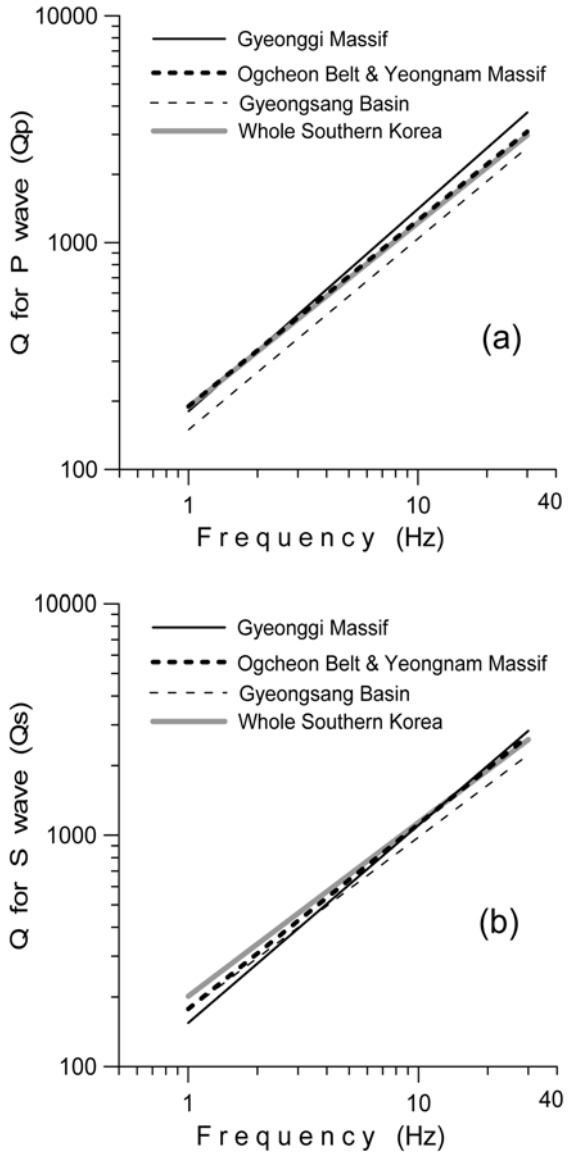

Fig. 7. Comparison of the frequency-dependent (a) Q_P and (b) Q_S for the whole southern Korean Peninsula and three sub-tectonic provinces.

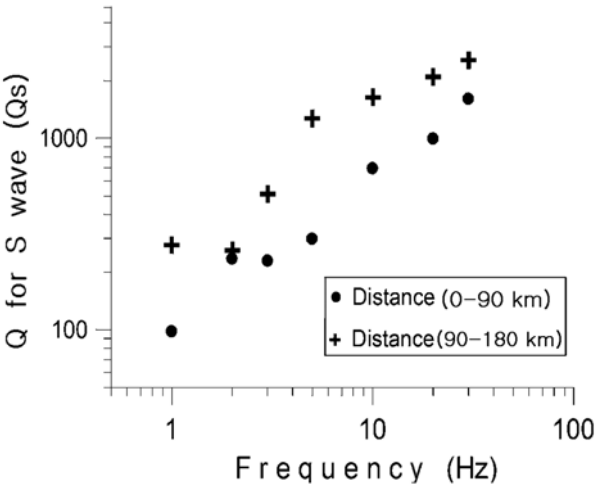

Fig. 8. Variation of frequency-dependent Q_S with the hypocentral distance. The values of Q_S at seven frequency pass bands (1, 2, 3, 5, 10, 20, and 30 Hz) are calculated. The result suggests that rays with longer (90-180 km) hypocentral distance penetrate the deeper crust and have a relatively high Q_S-value.

sula were estimated as a function of frequency as shown in Figures 5 and 6, respectively. Figure 7 compares the $Q_P(f)$ and $Q_S(f)$ for the southern Korean Peninsula and its sub-tectonic provinces.

We also analyzed the variation of frequency-dependent Q_S with two hypocentral distance ranges: 0–90 km and 90–180 km, respectively. The values of Q_S at seven frequency pass bands (1, 2, 3, 5, 10, 20, and 30 Hz) with the distance range of 90 to 180 km appear to be larger than those of the 0–90-km distance range, as shown in Figure 8. This suggests that rays with longer hypocentral distance penetrate the deeper crust and have a relatively high Q_S-value. This tendency has also been found in previous coda Q studies (Kim et al., 2000).

6. DISCUSSION

The values of Q and γ can be estimated simultaneously by the assumption of the frequency-independent Q from Equation (2) using multiple regression analysis. However, because the coefficients Q and γ are not fully independent of each other in Equation (1), a significant trade-off occurs between Q and γ in the inversion. In general, γ is assumed to be 1.0 for a short hypocentral distance within 100 km when the direct P_g and S_g phases arrive, and 0.5 for a distance beyond 100 km when L_g and surface waves are dominant (Chun et al., 1987; Shin and Hermann, 1987; Petukhin et al., 2003). However, some researchers regarded γ to be a constant (Rogers et al., 1987; Brockman and Bollinger, 1992). Others treated γ to be a variable depending on the propagation distance (Atkinson and Mereu, 1992; Kim et al., 2002; Atkinson 2004; Singh et al., 2004). Here, we treated γ as a variable in estimating the frequency-independent Q, while γ was assumed to be 1.0 in estimating the frequency-dependent Q, as done in other previous studies.

Table 1 lists the frequency-independent Q estimated for the sub-tectonic provinces. Kim et al. (1999) obtained a Q_P-value of 1686 in the Gyeongsang Basin; this value is significantly large compared to results of the present study. The value cannot be compared with our results because in determining Q_P, the spectral ratio of P to S waves was assumed to be 2.25, as expected in an ideal isotropic medium but questionable for the Korean Peninsula. Kim et al. (2000) also

estimated frequency-independent Q_P to be 625 in the Gyeongsang Basin, which is much smaller than the value obtained in the present study. The value of 625 was obtained from the initial pulse width method of P motion proposed by Stacey et al. (1975). Kim et al. (2000) assumed the constant related to the property for the earth medium in the method to be 0.5. The small value of Q_P may originate from the assumption of the ambiguous constant. Otherwise, the value may reflect the use of records having a shorter hypocentral distance than those used in the present study. In contrast, Cho and Baag (2003) estimated values of Q_S and γ for the Gyeongsang Basin as 1820 and 0.87, respectively, and these results coincide well with our results.

Among the linear trend of the frequency-dependent $Q_P(f)$ in sub-tectonic provinces shown in Figure 7(a), the Gyeonggi Massif and Ogcheon Belt show similar values in the low frequency range; however, the Gyeonggi Massif has a larger value than the Ogcheon Belt in the high frequency range. The Gyeongsang Basin shows the lowest value among the provinces. In the frequency-dependent relation of $Q_S(f)$ shown in Figure 7(b), the Ogcheon Belt and Gyeongsang Basin have similar values, and the Gyeonggi Massif has the smallest value in the low frequency range. In the high frequency range, the Gyeonggi Massif and the Ogcheon Belt have similar values, and the Gyeongsang Basin has the smallest value. It is noteworthy that the estimated Q-values for both P and S waves in the Gyeongsang Basin are the lowest, except for the case of $Q_S(f)$, in the low frequency range.

Some studies of Q_P and Q_S in the Korean Peninsula (Chung and Sato, 2001a; Chung et al., 2001; Kim et al., 2004) have used the coda-normalization method, and the resulting Q-values resemble those of other seismically stable regions such as the continental shield. Figure 9 compares frequency-dependent $Q_P(f)$ obtained in the present study with those of Chung and Sato (2001a) for the Gyeongsang Basin and Yoshimoto et al. (1993) for the Kanto region of Japan. There are minor differences in $Q_P(f)$ between the present study and Chung and Sato (2001a). The $Q_P(f)$ in the present study was significantly higher than that found by Yoshimoto et al. (1993) for a seismically active region. For comparison, Figure 10 shows the values for $Q_S(f)$ obtained in seismically active and stable areas. Although the frequency ranges treated in each study were not identical, such comparisons are possible. The $Q_S(f)$ estimated in this study is nearly the same as that by Chung and Sato (2001a). Furthermore, the $Q_S(f)$ in this study is comparatively higher than values found by Yoshimoto et al. (1993) for Kanto region of Japan and Raoof et al. (1999) for California of North America and lower than that found by Atkinson (2004) for Canada and northeastern United States.

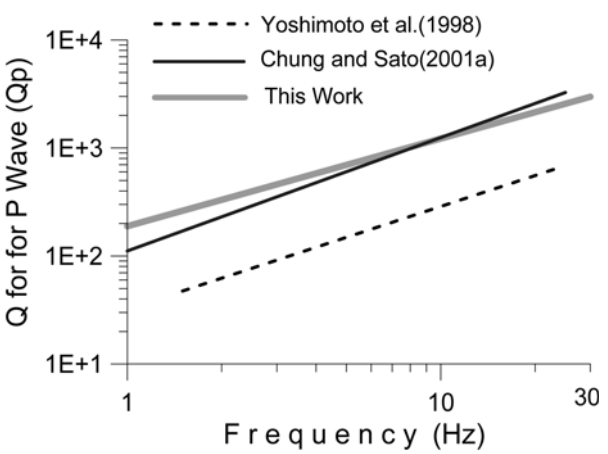

Fig. 9. Comparison of frequency-dependent Q_P values among studies. Chung and Sato (2001a) is for the Gyeongsang Basin of Korea, whereas Yoshimoto et al. (1993) is for the Kanto region of Japan. The $Q_P(f)$ in the southern Korean Peninsula is significantly higher than that of the seismically active Kanto region of Japan.

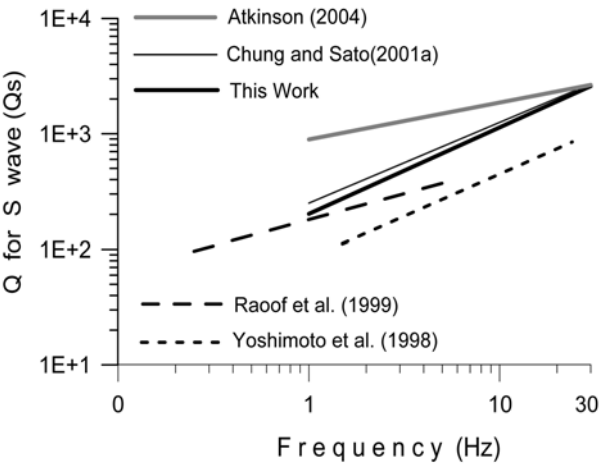

Fig. 10. Comparison of frequency-dependent Q_S values in seismically active and stable areas. The southern Korean Peninsula (this study) including Gyeongsang Basin (Chung and Sato, 2001a) and the northeastern United States (Atkinson, 2004) are known as seismically stable areas, whereas the Kanto region of Japan (Yoshimoto et al., 1993) and California of North America (Raoof et al., 1999) are seismically active areas. The $Q_S(f)$ in the southern Korean Peninsula is comparatively higher than values obtained in seismically active areas.

7. CONCLUSIONS

The Q_P and Q_S-values for the entire southern Korean Peninsula and three sub-tectonic provinces were determined using 675 seismograms from 191 local earthquakes. The frequency-independent values of Q_P and Q_S were estimated to be 1384 and 2036, respectively; the lowest values of Q_P and Q_S were observed in the Gyeongsang Basin. The geometric spreading factor γ varied from 0.75 to 0.86. The fre-

quency-dependent Q-value with the constant γ at the seven central frequencies (1, 2, 3, 5, 10, 20, and 30 Hz) was estimated to be $Q_P = 188.6 f^{0.8110}$ and $Q_S = 201.4 f^{0.7509}$ for the southern Korean Peninsula.

A significantly larger Q-value was found for the hypocentral distance range of 90 to 180 km than for the shorter hypocentral distance range, indicating that a seismic ray with a longer hypocentral distance passes through the deep crust having a relatively large Q-value. The $Q_S(f)$ estimated in this study was higher than for a seismically active area but lower than a seismically stable area.

ACKNOWLEDGEMENTS: This work was funded by the Korea Meteorological Administration Research and Development Program under Grant CATER_2006-5105.

REFERENCES

Aki, K., 1980, Attenuation of shear waves in the lithosphere for frequency from 0.05 to 25 Hz. Physics of the Earth and Planetary Interiors, 21, 50–60.

Aki, K. and Chouet, B., 1975, Origin of coda-waves: Source, attenuation, and scattering effects. Journal of Geophysical Research, 80, 3322–3342.

Atkinson, G.M., 2004, Empirical attenuation of ground-motion spectral amplitudes in southeastern Canada and the northeastern United States. Bulletin of the Seismological Society of America, 94, 1079–1095.

Atkinson, G.M. and Mereu, R.F., 1992, The shape of ground motion attenuation curves in southeastern Canada. Bulletin of the Seismological Society of America, 82, 2014–2031.

Brockman, S.R. and Bollinger, G.A., 1992, Q estimates along the Wasatch Front in Utah derived from Sg and Lg wave amplitudes. Bulletin of the Seismological Society of America, 82, 135–147.

Cho, N.D. and Baag, C.E., 2003, Estimation of spectrum decay parameter κ and stochastic prediction of strong ground motions in southeastern Korea. Bulletin of the Earthquake Engineering Society of Korea, 7, 59–70. (in Korean with English Abstract)

Chun, K.Y., West, G.F., Kokoski, R.J. and Samson, C., 1987, A novel technique for measuring Lg attenuation—Results from eastern Canada between 1 to 10 Hz. Bulletin of the Seismological Society of America, 77, 398–419.

Chung, T.W. and Sato, H., 2000, A study on the attenuation of high-frequency P and S waves in the crust of southeastern South Korea using the seismic data in Deok-jung Ri. Journal of Korean Geophysical Society, 3, 193–200. (in Korean with English abstract)

Chung, T.W. and Sato, H., 2001a, Attenuation of high-frequency P and S waves in the crust of southeastern South Korea. Bulletin of the Seismological Society of America, 91, 1867–1874.

Chung, T.W. and Sato, H., 2001b, A preliminary study on the attenuation of high-frequency P and S waves in the crust of the Yangsan fault area, southeastern South Korea. Science Reprint of Tohoku University (Series 5), 36, 291–294.

Chung, T.W., Sato, H. and Lee, K., 2001, A study of Q_P^{-1} and Q_S^{-1} based on data of 9 station in the crust of the southeastern Korea using extended coda normalization method. Journal of Korean Earth Sciences Society, 22, 500–511. (in Korean with English abstract)

Hino, M., 1986, Spectral Analysis. Asakura-Shoten, Tokyo, 300 pp. (in Japanese)

Kim, K.D., Chung, T.W., and Kyung, J.B., 2004, Attenuation of high-frequency P and S waves in the crust of the eastern part of Choongchung Province, central South Korea. Bulletin of the Seismological Society of America, 94, 1070–1078.

Kim, S.K., 1995, A study on the crustal structure of the Korean Peninsula. Journal of Geological Society of Korea, 31, 393–403. (in Korean with English abstract)

Kim, S.K., Jun, M.S. and Kim, J.K., 1999, Attenuation of P-wave in the Kyungsang Basin, southeastern Korea. Journal of Geological Society of Korea, 35, 223–228. (in Korean with English abstract)

Kim, S.K., Park, Y.K. and Jun, M.S., 2000, Quality factor structure of the southeastern part of the Korean Peninsula. Journal of Geological Society of Korea, 36, 529–544. (in Korean with English abstract)

Kim, S.K., Kim, S.K., and Chi, H.C., 2002, Attenuation of peak spectral amplitude of acceleration in the southern part of the Korean Peninsula. Journal of Geological Society of Korea, 38, 237–250. (in Korean with English abstract)

Petukhin, A., Irikura, K., Ohmi, S. and Kagawa, T., 2003, Estimation of Q-values in the seismogenic and aseismic layers in the Kinki Region, Japan, by elimination of the geometrical spreading effect using ray approximation. Bulletin of the Seismological Society of America, 93, 1498–1515.

Raoof, M., Herrmann, R.B. and Malagnini, L., 1999, Attenuation and excitation of three-component ground motion in southern California. Bulletin of the Seismological Society of America, 89, 888–902.

Reedman, A.J. and Um, S.H., Geology of Korea. Korea Institute of Energy and Resources, Seoul, 139p.

Rogers, A.M., Harmsen, S.C., Hermann, R.B. and Meremonte, M.E., 1987, A study of ground motion in the Southern Great Basin, Nevada–California, using several techniques for estimation of Qs, log Ao, and Coda Q. Journal of Geophysical Research, 92, 3527–3540.

Shin, T.C. and Hermann, R.B., 1987, Lg attenuation and source studies using 1982 Miramichi data. Bulletin of the Seismological Society of America, 77, 384–397.

Singh, S.K., Garcia, D., Pacheco, J.F., Valenzuela, R. Bansal, B.K. and Dattatrayam, R.S., 2004, Q of the Indian Shield. Bulletin of the Seismological Society of America, 94, 1564–1570.

Stacey, F.D., 1977, Physics of the earth, John Wiley & Sons, New York, 414 p.

Stacey, F.D., Gladwin, M.T., Mckavanagh, B., Linde, A.T. and Hastic, L.M., 1975, Anelastic damping of acoustic and seismic pulses. Geophysical Survey, 2, 133–157.

Yoshimoto, K., Sato, H. and Ohtake, M., 1993, Frequency-dependent attenuation of P and S waves in the Kanto area, Japan, based on the coda-normalization method. Geophysical Journal International, 114, 165–174.

Manuscript received April 6, 2005
Manuscript accepted December 5, 2006

Appendix 1. The list of earthquakes used in this study (KIGAM = Korea Institute of Geoscience & Mineral Resources; KMA = Korea Meteorological Administration).

Origine time		Latitude	Longitude	Depth	M_L	No. of	Data
yr/mon/day	hr:min:sec	(°N)	(°E)	(km)		Record	Source
00/01/20	07:05:58	35.7842	129.3868	10.78	1.5	1	KIGAM
00/01/21	10:17:58	35.7910	128.4868	7.24	2.4	1	KIGAM
00/02/16	19:05:51	35.8103	127.9392	6.30	2.6	2	KIGAM
00/02/21	01:06:31	35.8073	128.2672	5.31	2.1	9	KIGAM
00/02/21	20:27:35	35.8117	128.2657	4.18	2.4	5	KIGAM
00/03/04	18:24:35	35.0925	129.6923	14.93	2.8	4	KIGAM
00/03/09	16:30:25	35.9025	129.6177	17.86	1.8	3	KIGAM
00/03/10	18:47:27	35.9940	129.5622	5.38	2.0	1	KIGAM
00/03/11	12:27:10	36.0000	129.0733	5.84	1.8	2	KIGAM
00/03/13	08:07:33	34.7912	128.5512	12.76	2.7	2	KIGAM
00/03/15	01:10:52	36.3000	125.9000	1.00	2.5	1	KMA
00/03/19	16:46:14	36.8450	129.8732	6.06	2.8	4	KIGAM
00/03/21	13:43:56	36.3865	126.0762	19.51	2.8	3	KIGAM
00/04/10	23:47:43	34.1185	127.0243	18.41	3.2	1	KIGAM
00/01/00	20:05:39	35.0980	129.7798	12.40	2.4	5	KIGAM
00/04/13	10:40:57	36.6418	130.0683	0.74	2.8	7	KIGAM
00/04/15	08:05:19	36.5833	128.3103	8.62	2.9	8	KIGAM
00/04/29	08:53:27	35.8000	125.7000	29.28	3.3	1	KMA
00/05/09	06:55:36	35.2425	128.1493	11.27	2.3	10	KIGAM
00/05/11	00:52:44	36.2690	128.5132	12.86	2.6	7	KIGAM
00/05/17	17:42:08	35.8481	129.2612	8.32	1.9	1	KIGAM
00/05/19	01:44:24	36.3075	128.5028	11.29	2.7	10	KIGAM
00/05/26	21:41:41	36.1545	127.1923	0.35	2.4	7	KIGAM
00/05/31	15:36:43	34.4573	127.1512	7.55	2.8	3	KIGAM
00/06/04	13:42:45	35.9015	129.6118	18.17	2.4	2	KIGAM
00/06/06	00:14:40	35.5240	128.3550	1.12	2.2	3	KIGAM
00/06/16	09:16:03	35.8788	129.7030	18.29	2.0	3	KIGAM
00/08/05	21:03:00	34.5815	125.3757	5.34	2.7	2	KIGAM
00/08/06	19:35:09	36.3000	128.4000	2.93	2.2	1	KMA
00/08/15	01:36:30	35.3000	125.9000	5.53	2.2	3	KMA
00/08/21	19:43:38	38.8938	125.7765	10.00	3.6	1	KIGAM
00/09/23	10:07:45	35.6000	128.4000	20.39	2.4	3	KMA
00/10/03	07:46:37	37.3000	128.8000	10.00	2.6	1	KMA
00/11/05	21:39:41	36.2000	127.2000	10.00	2.2	1	KMA
01/01/13	16:53:40	34.6000	126.9000	10.00	3.1	3	KMA
01/01/13	07:47:12	35.6892	129.8677	23.84	2.3	3	KIGAM
01/01/29	11:44:09	35.6533	126.6458	0.60	3.5	4	KIGAM
01/02/03	13:42:14	36.1052	129.5800	4.61	1.8	2	KIGAM
01/02/10	16:23:28	35.8433	129.2452	5.97	2.4	3	KIGAM
01/02/14	01:02:08	36.0190	128.2447	0.45	2.6	7	KIGAM
01/03/06	00:23:05	35.3000	125.7000	1.70	2.3	3	KMA
01/03/12	12:02:28	36.8163	129.5472	10.00	2.5	1	KIGAM
01/04/16	22:50:32	35.9000	129.7000	13.66	2.2	5	KIGAM
01/04/17	02:42:50	35.4000	126.1000	6.29	2.5	6	KMA

Appendix 1. Continued.

Origine time		Latitude	Longitude	Depth	M_L	No. of	Data
yr/mon/day	hr:min:sec	(°N)	(°E)	(km)		Record	Source
01/04/21	02:30:46	35.8705	125.2300	5.00	2.6	1	KIGAM
01/05/01	02:43:45	35.9987	129.7532	14.76	2.3	3	KIGAM
01/05/05	19:23:46	34.4000	127.4000	28.29	1.7	2	KMA
01/05/14	05:11:43	35.9444	129.9260	22.19	2.1	3	KIGAM
01/05/16	01:09:04	35.9555	126.7697	3.36	2.5	7	KIGAM
01/05/25	00:06:25	33.6000	126.8000	10.00	2.6	1	KMA
01/05/27	20:24:02	35.8000	129.7000	16.05	2.5	3	KMA
01/05/28	07:25:06	36.4000	127.8000	10.00	2.1	2	KMA
01/06/09	00:36:12	36.7412	128.8392	8.20	2.4	3	KIGAM
01/06/16	21:26:02	36.0000	127.9000	10.00	2.2	3	KIGAM
01/06/17	01:04:25	35.7000	126.4000	10.00	2.3	2	KMA
01/06/24	08:19:44	35.8233	129.6692	12.86	2.8	2	KMA
01/06/29	11:21:08	35.8000	126.6000	5.59	3.6	3	KMA
01/07/15	20:01:47	36.8978	127.2245	10.00	2.7	3	KIGAM
01/07/22	01:59:11	36.5028	127.9163	8.09	2.5	6	KIGAM
01/07/27	10:04:39	36.4500	127.9658	1.06	2.4	6	KIGAM
01/08/06	23:46:44	36.6960	128.3933	6.67	2.4	4	KIGAM
01/08/20	10:59:36	35.2215	129.2655	1.49	2.4	2	KIGAM
01/08/24	06:08:41	36.1100	127.5793	2.58	1.9	4	KIGAM
01/08/26	03:48:02	36.7142	127.2068	2.10	1.9	1	KIGAM
01/09/13	06:07:15	36.4000	127.0000	5.32	2.2	3	KMA
01/09/15	02:32:42	35.6000	125.9000	10.00	2.2	2	KMA
01/09/16	09:05:42	35.7055	129.3537	8.69	2.0	1	KIGAM
01/09/19	08:47:57	36.6000	126.9000	7.19	2.6	5	KMA
01/09/24	09:33:31	35.5000	127.5000	0.31	2.6	2	KMA
01/10/01	03:35:52	36.0132	127.6563	6.80	3.0	5	KIGAM
01/10/03	01:42:50	37.1225	128.8000	0.16	2.0	2	KIGAM
01/10/22	04:37:51	35.8527	129.6262	15.44	2.4	3	KIGAM
01/10/26	08:57:42	35.7842	129.3792	11.16	2.4	3	KIGAM
01/10/31	05:03:39	36.0393	126.6450	0.05	2.3	3	KIGAM
01/11/09	13:54:47	34.7000	126.9000	10.00	2.6	1	KIGAM
01/11/13	06:15:20	36.5000	127.9000	2.50	1.9	5	KMA
01/11/21	10:49:12	36.6962	128.3432	0.52	3.6	8	KIGAM
01/11/24	16:10:32	36.7320	129.8523	7.07	4.1	6	KIGAM
01/11/30	11:18:32	35.9000	127.5000	6.63	2.4	2	KMA
01/12/16	16:25:05	36.3715	127.0533	2.39	2.2	2	KIGAM
02/01/04	00:33:23	36.8258	127.2155	2.20	2.2	4	KIGAM
02/01/07	17:10:00	35.4000	128.8000	5.00	3.1	5	KMA
02/01/08	08:18:31	35.8000	128.2000	14.36	2.8	3	KMA
02/01/13	00:50:43	36.3100	128.5338	0.08	2.1	4	KIGAM
02/01/17	06:28:27	36.2000	126.2000	9.15	2.8	2	KMA
02/02/01	07:10:00	36.2940	129.0117	9.69	2.1	4	KIGAM
02/02/02	00:32:20	35.6220	130.0670	5.00	2.1	2	KIGAM
02/02/03	22:44:11	34.9920	125.1287	0.14	2.8	1	KIGAM

Appendix 1. Continued.

Origine time		Latitude	Longitude	Depth	M_L	No. of	Data
yr/mon/day	hr:min:sec	(°N)	(°E)	(km)		Record	Source
02/02/06	12:23:37	36.6125	128.7797	0.07	2.3	6	KIGAM
02/02/07	09:31:16	36.1000	129.2000	20.70	2.4	7	KMA
02/02/10	04:27:22	37.0570	128.9747	1.36	2.1	1	KIGAM
02/02/15	11:26:32	36.5262	128.1632	7.69	2.3	5	KIGAM
02/02/22	10:56:35	36.7132	127.1958	2.34	2.3	2	KIGAM
02/02/28	22:26:49	36.6367	128.0767	0.46	2.2	1	KIGAM
02/03/02	10:47:15	36.6450	128.1032	2.29	2.4	3	KIGAM
02/03/07	23:30:57	36.4492	126.6072	0.26	3.2	6	KIGAM
02/03/08	02:09:33	35.5000	126.1000	5.00	2.4	2	KMA
02/03/11	05:45:55	34.7588	127.8652	5.00	2.1	2	KIGAM
02/03/12	20:04:37	34.9000	127.4000	10.00	2.4	2	KMA
02/03/17	09:26:38	38.1040	124.5605	0.60	3.8	1	KIGAM
02/03/25	05:31:06	37.4000	129.2000	0.54	2.4	3	KMA
02/03/25	18:10:26	37.1000	127.2000	0.68	2.4	2	KMA
02/03/29	19:24:18	35.0423	129.6362	0.19	2.3	3	KIGAM
02/03/31	07:58:41	38.5192	127.7470	13.20	2.6	1	KIGAM
02/04/01	07:46:02	37.3000	128.1000	0.27	2.5	8	KMA
02/04/06	22:33:18	34.7120	129.4448	2.65	2.0	1	KIGAM
02/04/09	16:14:12	36.0000	129.5740	5.28	1.8	3	KMA
02/04/14	12:30:01	35.0457	125.1077	1.59	2.8	1	KIGAM
02/04/15	08:36:07	35.8927	129.6517	12.25	2.2	3	KIGAM
02/04/24	07:32:08	35.3075	126.1967	19.48	2.2	1	KIGAM
02/04/29	05:50:59	37.3562	129.4720	0.65	2.4	2	KIGAM
02/05/02	07:18:23	35.5550	129.8818	9.29	2.0	3	KIGAM
02/05/13	18:38:14	34.7465	128.8845	2.50	2.3	2	KIGAM
02/05/14	09:14:41	34.1222	129.2125	0.54	3.3	2	KIGAM
02/05/17	12:06:09	38.7920	126.1348	8.71	2.3	1	KIGAM
02/05/21	14:42:17	35.7267	128.7040	5.00	1.7	2	KIGAM
02/05/22	19:07:56	38.3928	127.7395	5.00	2.6	2	KIGAM
02/05/23	22:11:21	35.1153	129.8627	0.25	2.1	4	KIGAM
02/05/25	23:44:22	35.1085	129.7460	2.44	2.1	6	KIGAM
02/05/29	18:22:17	34.6358	127.8532	5.00	2.5	10	KIGAM
02/05/30	18:18:27	36.4555	125.7800	0.18	2.7	1	KIGAM
02/06/07	22:24:14	38.7025	125.6377	0.31	3.2	1	KIGAM
02/06/11	22:13:41	35.8550	129.5400	12.83	2.5	3	KIGAM
02/06/21	05:31:35	36.7848	128.7170	0.91	2.0	6	KIGAM
02/06/23	11:12:57	34.7000	126.6000	10.00	2.0	2	KMA
02/06/27	15:29:13	36.0025	129.5650	0.48	2.1	2	KIGAM
02/07/02	01:49:07	35.8000	128.0000	1.50	2.3	8	KMA
02/07/08	13:34:02	36.5402	128.0757	5.48	2.3	5	KIGAM
02/07/09	04:01:50	35.8608	129.7915	11.54	3.7	8	KIGAM
02/07/12	08:17:29	35.8550	129.7190	12.83	2.5	5	KIGAM
02/07/17	06:50:31	37.9760	125.1647	0.84	3.4	1	KIGAM
02/08/06	07:32:40	34.6965	127.3998	7.92	3.8	10	KIGAM

Appendix 1. Continued.

Origine time		Latitude	Longitude	Depth	M_L	No. of	Data
yr/mon/day	hr:min:sec	(°N)	(°E)	(km)		Record	Source
02/08/23	08:37:56	38.4197	127.7768	5.95	2.5	1	KIGAM
02/08/26	05:24:54	36.1316	126.0823	0.48	2.3	2	KIGAM
02/08/29	08:25:58	35.9855	129.7335	5.00	1.7	2	KIGAM
02/09/04	02:58:26	35.2397	129.0482	0.56	1.9	1	KIGAM
02/09/06	14:53:26	34.2210	129.8293	0.46	2.8	2	KIGAM
02/09/10	15:36:36	34.8968	130.1687	15.26	2.3	4	KIGAM
02/09/15	16:40:02	35.8648	129.6953	11.43	2.7	12	KIGAM
02/09/16	07:36:07	36.1000	128.3000	10.09	2.8	7	KMA
02/09/19	03:10:13	35.6000	125.4000	0.39	2.9	4	KMA
02/10/04	02:06:31	38.1000	126.4000	5.73	2.4	2	KMA
02/10/16	19:48:59	36.6000	127.6000	9.74	2.4	10	KMA
02/10/19	21:31:55	36.1463	127.5862	13.06	2.6	5	KMA
02/10/20	04:22:08	35.2000	127.7000	9.65	3.0	6	KIGAM
02/10/23	10:30:54	34.8862	128.4612	3.51	3.2	7	KMA
02/10/24	21:01:34	35.8478	129.6683	16.43	1.9	6	KIGAM
02/10/25	04:06:49	33.9687	127.1358	5.00	2.9	5	KIGAM
02/10/28	11:50:53	35.0662	126.6688	5.00	3.0	9	KIGAM
02/10/29	03:02:23	35.8737	129.1442	8.69	1.5	3	KIGAM
02/11/06	21:48:07	36.4000	127.7000	5.00	2.5	10	KMA
02/11/13	21:46:26	35.8000	127.9000	10.00	2.4	1	KMA
02/12/05	10:05:46	36.7640	126.2877	10.39	2.6	2	KIGAM
02/12/07	16:43:38	37.4000	129.5000	5.00	2.7	2	KMA
02/12/12	21:42:22	37.1000	126.4000	0.68	2.3	3	KMA
02/12/16	18:21:39	36.6742	130.0352	12.32	2.5	3	KIGAM
02/12/17	08:44:56	37.1257	126.4855	8.10	2.5	3	KIGAM
02/12/26	23:41:51	36.5542	127.0193	12.48	2.6	4	KIGAM
03/01/03	07:13:02	35.8528	129.6762	20.31	1.9	4	KIGAM
03/01/09	17:33:21	37.5338	124.5678	5.00	3.9	1	KIGAM
03/01/10	07:56:05	35.8128	129.2410	1.65	3.0	9	KIGAM
03/01/13	21:44:04	35.7110	129.3538	8.34	1.9	2	KIGAM
03/01/13	22:03:25	35.8000	129.4000	8.34	2.8	2	KMA
03/01/16	14:02:58	33.6000	127.3000	0.15	2.2	2	KMA
03/01/17	16:33:12	35.7368	129.3603	11.02	2.3	5	KIGAM
03/02/04	16:34:48	35.7238	129.4028	12.79	2.1	4	KIGAM
03/02/08	23:46:33	35.3893	126.6407	5.00	3.1	9	KIGAM
03/02/09	22:28:45	35.9855	127.8752	10.43	2.7	11	KIGAM
03/03/01	23:33:28	35.8000	129.3000	10.37	3.0	4	KMA
03/03/04	12:44:25	38.3000	128.6000	5.00	2.9	2	KMA
03/03/10	03:28:03	36.1000	128.4000	1.22	3.1	5	KMA
03/03/14	04:06:12	36.2000	128.7000	15.46	2.1	4	KMA

Appendix 1. Continued.

Origine time		Latitude	Longitude	Depth	M_L	No. of	Data
yr/mon/day	hr:min:sec	(°N)	(°E)	(km)		Record	Source
03/03/19	23:05:18	36.5000	129.6000	0.33	2.3	1	KMA
03/04/01	22:26:38	36.4000	127.8000	1.34	2.1	2	KMA
03/04/05	00:31:32	36.2000	127.3000	1.23	2.9	5	KMA
03/04/05	00:25:08	36.2000	127.3000	0.43	2.5	5	KMA
03/04/05	00:56:09	36.2000	127.3000	12.57	2.4	1	KMA
03/04/16	02:55:25	36.4000	126.3000	0.68	3.3	2	KMA
03/06/08	02:07:57	36.5000	125.1000	5.00	2.6	1	KMA
03/07/05	12:18:28	37.4000	125.3000	5.00	3.0	1	KMA
03/07/09	15:20:11	34.8660	128.2153	9.46	2.9	9	KIGAM
03/08/07	11:04:20	36.8000	129.5000	3.03	2.7	4	KMA
03/08/12	01:25:56	34.7000	130.3000	17.61	2.6	1	KMA
03/09/24	03:26:56	35.7861	128.4350	9.41	3.0	11	KIGAM
03/09/25	15:24:17	36.0000	129.6000	11.37	2.5	3	KMA
03/10/05	05:03:53	36.3000	127.3000	1.10	2.1	4	KMA
03/10/13	18:12:05	36.9715	126.4567	1.95	3.0	4	KIGAM
03/10/14	01:44:38	34.1000	127.5000	0.66	2.4	1	KMA
03/10/17	11:55:58	35.7040	129.3738	7.99	2.4	4	KIGAM